Original Article

MOLECULAR METABOLISM

Gsα-dependent signaling is required for postnatal establishment of a functional β-cell mass

Berta Serra-Navarro [1,2], Rebeca Fernandez-Ruiz [1,2,3], Ainhoa García-Alamán [1,3], Marta Pradas-Juni [1,2], Eduardo Fernandez-Rebollo [1,3], Yaiza Esteban [1,3], Joan Mir-Coll [1,2], Julia Mathieu [4], Stephane Dalle [4], Max Hahn [5], Ulf Ahlgren [5], Lee S. Weinstein [6], Josep Vidal [1,2,3,7], Ramon Gomis [1,2,3,8], Rosa Gasa [1,3,*]

ABSTRACT

Objective: Early postnatal life is a critical period for the establishment of the functional β-cell mass that will sustain whole-body glucose homeostasis during the lifetime. β cells are formed from progenitors during embryonic development but undergo significant expansion in quantity and attain functional maturity after birth. The signals and pathways involved in these processes are not fully elucidated. Cyclic adenosine monophosphate (cAMP) is an intracellular signaling molecule that is known to regulate insulin secretion, gene expression, proliferation, and survival of adult β cells. The heterotrimeric G protein Gs stimulates the cAMP-dependent pathway by activating adenylyl cyclase. In this study, we sought to explore the role of Gs-dependent signaling in postnatal β-cell development.

Methods: To study Gs-dependent signaling, we generated conditional knockout mice in which the α subunit of the Gs protein (Gsα) was ablated from β-cells using the Cre deleter line *Ins1*^{Cre}. Mice were characterized in terms of glucose homeostasis, including *in vivo* glucose tolerance, glucose-induced insulin secretion, and insulin sensitivity. β-cell mass was studied using histomorphometric analysis and optical projection tomography. β-cell proliferation was studied by ki67 and phospho-histone H3 immunostatining, and apoptosis was assessed by TUNEL assay. Gene expression was determined in isolated islets and sorted β cells by qPCR. Intracellular cAMP was studied in isolated islets using HTRF-based technology. The activation status of the cAMP and insulin-signaling pathways was determined by immunoblot analysis of the relevant components of these pathways in isolated islets. *In vitro* proliferation of dissociated islet cells was assessed by BrdU incorporation.

Results: Elimination of Gsα in β cells led to reduced β-cell mass, deficient insulin secretion, and severe glucose intolerance. These defects were evident by weaning and were associated with decreased proliferation and inadequate expression of key β-cell identity and maturation genes in postnatal β-cells. Additionally, loss of Gsα caused a broad multilevel disruption of the insulin transduction pathway that resulted in the specific abrogation of the islet proliferative response to insulin.

Conclusion: We conclude that Gsα is required for β-cell growth and maturation in the early postnatal stage and propose that this is partly mediated via its crosstalk with insulin signaling. Our findings disclose a tight connection between these two pathways in postnatal β cells, which may have implications for using cAMP-raising agents to promote β-cell regeneration and maturation in diabetes.

Keywords β-Cell mass; cAMP; Gs; Insulin signaling; Cell maturation; Postnatal development; Replication

1. INTRODUCTION

Pancreatic β cells secrete the blood-glucose-lowering hormone insulin and play a crucial role in controlling whole-body glucose homeostasis. A deficit in the number of functional β cells leads to insulin deficiency, elevated blood glucose levels, and the emergence of diabetes. Regenerative medicine strategies aimed to replace lost or dysfunctional β cells are currently viewed as promising therapies to treat this disease. Some approaches propose endogenous β cell regeneration by stimulating the proliferation/survival of residual β cells, whilst others propose transplantation of substitute β cells created in the laboratory from other cell sources. Progress on these two fronts relies on our

[1]Diabetes and Obesity Research Laboratory, August Pi i Sunyer Biomedical Research Institute (IDIBAPS), Rosselló 149-153, 08036, Barcelona, Spain [2]University of Barcelona, Barcelona, Spain [3]Centro de Investigación Biomédica en Red de Diabetes y Enfermedades Metabólicas Asociadas (CIBERDEM), Spain [4]CHU Montpellier, Laboratory of Cell Therapy for Diabetes (LTCD), Hospital St-Eloi, Montpellier, France [5]Umeå Centre for Molecular Medicine (UCMM), Umeå, Sweden [6]Metabolic Diseases Branch, National Institute of Diabetes, Digestive, and Kidney Diseases, NIH, Bethesda, MD, USA [7]Department of Endocrinology and Nutrition, Hospital Clinic of Barcelona, Barcelona, Spain [8]Universitat Oberta de Catalunya (UOC), Barcelona, Spain

*Corresponding author. Diabetes and Obesity Research Laboratory, August Pi i Sunyer Biomedical Research Institute (IDIBAPS), Rosselló 149-153, 08036, Barcelona, Spain. E-mail: rgasa@clinic.cat (R. Gasa).

Abbreviations: Gsα, Stimulatory G protein (Gs) alpha subunit; Giα, Inhibitory G protein (Gi) alpha subunit; cAMP, Cyclic adenosine monophosphat; GPCR, G protein coupled receptor; Igf, Insulin-like growth factor

Received March 18, 2021 • Revision received May 17, 2021 • Accepted May 30, 2021 • Available online 4 June 2021

https://doi.org/10.1016/j.molmet.2021.101264

knowledge of agents and molecular pathways amenable to be manipulated to promote β-cell expansion and/or to achieve β cell functional maturation.

Early postnatal life is a critical period for acquiring the appropriate number of functional β cells needed to sustain the metabolic needs of the adult organism [1]. The β-cell population expands dramatically during the perinatal period due to increased proliferation [2–4], which rapidly declines until reaching low replication values maintained throughout adulthood (cells in cycle: ≈1% in rodents and <0.2% in humans) [5]. In concert with their expansion, neonatal β cells up-regulate the expression of identity and functionality genes and develop the capability to regulate insulin secretion in response to high glucose (GSIS), which is the hallmark of their mature state [6–9]. Therefore, early postnatal life (in mice, between birth and weaning) is a critical period in β-cell development that can provide information on the identity of central regulators of β-cell growth and function.

Cyclic adenosine monophosphate (cAMP) is a common and versatile intracellular signaling molecule. In β cells, cAMP has been implicated in the stimulus-insulin secretion coupling process [10–12], in the expression of key β-cell markers such as Insulin and the transcription factors Pdx1 and Mafa [13–15], as well as in β-cell proliferation and survival [16–20]. cAMP is generated from ATP by adenylyl cyclases, which can be regulated by G-protein coupled receptors (GPCRs) that either stimulate this enzyme via Gsα or inhibit it via Giα subunits. Genetic approaches that disrupt these subunits have evidenced their involvement in the regulation of β-cell mass. Thus, deletion of the gene encoding Gsα in mouse pancreatic β cells using the Rat Insulin Promoter 2 (RIP2)-Cre transgene resulted in reduced β-cell mass, deficient insulin secretion and whole-body glucose intolerance in adult mice [21]. Conversely, inhibition of Gi/oα through the expression of the Pertussis toxin in β cells led to increased β-cell mass, augmented insulin secretion, and improved glucose tolerance [22]. In both models, the β-cell mass phenotype appeared during the early postnatal stage and was associated with altered β-cell proliferation. However, neither the mechanisms involved nor the effects on postnatal β-cell maturation were explored.

Here we sought to investigate the involvement of Gsα-dependent signaling in postnatal β-cell development in detail. To ablate the *Gnas* gene (i.e., codes for Gsα) from β cells, we used *Ins1*^{Cre} knock-in mice, which present highly selective induction of Cre-dependent recombination in β cells [23]. Because the *RIP2*-Cre line used before is known to drive significant non-β-cell Cre expression, namely in the hypothalamus and pituitary [24], and to display transgene-related β-cell dysfunction [25], we reasoned that using *Ins1*^{Cre} deleter mice should lead to unambiguous insights into the role of Gsα signaling in postnatal β cells. Our study demonstrates that the specific elimination of Gsα in β cells results in hyperglycemia and whole-body glucose intolerance. This metabolic phenotype is associated with a compromised postnatal functional β-cell mass establishment and entails both reduced β-cell expansion and deficient β-cell maturation. Mechanistically, we show that Gsα ablation leads to severe depletion of intracellular cAMP levels, reduced Creb activation, and multilevel dysregulation of the insulin transduction pathway in postnatal β cells.

2. METHODS

2.1. Mice

Mice with loxP sites surrounding Gsα exon 1 (*Gnas*$^{flox/flox}$) [26], Ins1(Cre) knock-in mice [23], and ROSA26-Stop-EYFP mice [27] were described elsewhere. Female *Gnas*$^{flox/flox}$ mice were mated to male *Gnas*$^{flox/+}$;*Ins1*$^{Cre/+}$ mice to generate Gsα knockout mice (*Gnas*$^{flox/flox}$;*Ins1*$^{Cre/+}$). As controls, we used littermates with *Gnas*$^{flox/flox}$;*Ins1*$^{+/+}$ and *Gnas*$^{flox/+}$; *Ins1*$^{+/+}$ genotypes, except for β-cell sorting experiments, where we used *Gnas*$^{flox/+}$;*Ins1*$^{Cre/+}$ and *Gnas*$^{+/+}$;*Ins1*$^{Cre/+}$. Experimental procedures and postnatal tissues were collected at the indicated times, considering birth the postnatal day 0 (p0). Mice were bred and maintained on a standard pellet diet (2014S Teklad Global, Harlan Laboratories) and 12:12 h light/dark cycle at the barrier animal facility of the University of Barcelona. Principles of laboratory animal care were followed (European and local government guidelines), and animal experimental procedures were approved by the Animal Research Committee of the University of Barcelona. Animals were euthanized by cervical dislocation. Genotyping for mice was performed by PCR on tail DNA using primers supplied in Supplementary Table S1. The PCR was carried out using DreamTaq DNA polymerase (Thermo Fisher Scientific, Waltham, US), and the reaction was performed by denaturation at 95 °C for 3 min and 35 cycles of amplification (95 °C for 30 s, 60 °C for 30 s, 72 °C for 1 min), finishing with 10 min at 72 °C.

2.2. Whole-body metabolic tests

The Intraperitoneal and Oral Glucose Tolerance Tests were performed after 6 h of food deprivation by the administration of D-glucose (2 g/kg body weight) via intraperitoneal injection or by oral gavage, respectively. The Insulin Tolerance Test was performed after 6 h of food deprivation by the administration of an injection of insulin (Humulin; 0.5 U/kg body weight). Glucose levels in tail vein blood samples were measured at 0, 15, 30, 60, and 120 min after injection using a clinical glucometer and Accu–Check test strips (Roche Diabetes Care, Sant Cugat, Spain). Glucose-stimulated insulin secretion (GSIS) was measured in 5–6 h fasted mice following an intraperitoneal injection of glucose (3 mg/kg body weight). Tail vein blood was collected in heparinized capillary tubes (Microvette, Sarstedt, Nümbrecht, Germany) at indicated time points. Plasma insulin concentration was measured using the Ultrasensitive Mouse Insulin ELISA (Chrystal Chem, Zaandam, Netherlands). Plasma proinsulin levels were measured with the highly specific Mouse Proinsulin ELISA (Mercodia, Uppsala, Sweden).

2.3. Islet isolation and culture

Islets were isolated by collagenase digestion (Collagenase P, Roche Diagnostics GmbH, Mannheim, Germany) and discontinuous Histopaque (Sigma–Aldrich, Steinheim, Germany) gradient centrifugation (p28 and adult mice) [28] or manual handpicking under a stereomicroscope (p7 mice). The collagenase solution (0.7 mg/ml) was injected into the common bile duct in p28 and adult animals or multi-injected at a concentration of 0.5 mg/ml in the pancreas of p7 mice. After isolation, islets were either used fresh or transferred to dishes containing an RPMI-1640 medium (Sigma–Aldrich) with 11 mM of glucose, 10% fetal bovine serum (FBS) (Biosera, Nuaille, France), 2 mM L-glutamine, and HyClone™ Penicillin-Streptomycin (100 U/ml penicillin, 100 pg/ml streptomycin; GE Healthcare Life Sciences, PGH, USA) for a 16–24 h recovery culture before performing additional procedures.

2.4. Purification of β cells by fluorescence activated cell sorting

Freshly isolated islets from p28 *Gnas*$^{flox/flox}$;*Ins1*$^{Cre/+}$;R26-YFP and *Gnas*$^{+/+}$;*Ins1*$^{Cre/+}$;R26-YFP or *Gnas*$^{flox/+}$;*Ins1*$^{Cre/+}$;R26-YFP mice were dispersed with 0.125% trypsin-EDTA (Life Technologies-ThermoFisher Scientific) and 50 ng/ml Dnase I (Stem cell Technologies, Égrève, France) with agitation for 9–12 min at 37 °C. Digestion was inactivated by the addition of 0.4 volumes of FBS. Dispersed islets were collected in 15 ml tubes, pelleted, and resuspended to a concentration of ~2 × 10^6 cells/ml in RPMI+10%FBS. Sorting was

performed using a BD FACSariaII (for YFP) machine, and cells were recovered in RNA lysis buffer for RNA extraction.

2.5. Gene expression

Total RNA was prepared from isolated islets using the NucleoSpin XS RNA kit (Mackerey-Nagel, Düren, Germany). First-strand cDNA was prepared using the Superscript III RT kit and random hexamer primers (Invitrogen, Carlsbad, CA, USA). Reverse transcription reaction was carried for 90 min at 50 °C and an additional 10 min at 55 °C. Quantitative real-time PCR (qPCR) was performed on an ABI Prism 7900 sequence detection system using GoTaq® qPCR Master Mix (Promega Biotech Ibérica, Alcobendas, Madrid, Spain). Expression relative to a housekeeping gene was calculated using the deltaCt method. We picked the moderately expressed gene *Tbp* as housekeeping for all the genes except for the pancreatic hormones and *Iapp*, which are more abundant and whose expression was compared to that of *Actb*.

Conventional PCR was performed on 10 ng of islet cDNA in 20 μl reactions containing DreamTaq Green PCR Mastermix (Thermo Fisher Scientific) and 0.5 μM forward and reverse primers. PCR conditions were as follows: 95 °C for 3 min, then 35 cycles of 95 °C for 15 s, 60 °C for 15 s, 72 °C for 45 s followed by 10 min at 72 °C. PCR products were separated on 3% low-melting agarose gel. All primer sequences are provided in Supplementary Table S1.

2.6. Immunofluorescence and morphometric analysis

Pancreases from p14, p28, and adult mice were fixed in 4% formalin overnight at 4 °C. Pancreases from p0 mice were fixed in 4% paraformaldehyde (PFA) (Electron Microscopy Sciences, Hatfield, PA) for 5–6 h. After fixation, pancreases were washed, dehydrated, embedded in paraffin wax, sectioned at 3 μm, and stained following standard inmunodetection protocols [29]. Briefly, tissues were rehydrated and, when required, subject to heat-mediated antigen retrieval in a citrate buffer. After a blocking step in 5% donkey serum/0.2% Triton X-100, sections were incubated overnight with primary antibodies: guinea pig anti-insulin (1:1000 dilution, Dako, Glostrup, Denmark), mouse anti-glucagon (1:1000 dilution, Dako), chicken anti-GFP (1:200, Abcam), rabbit anti-MafA (1:250, Novus Biologicals, Centennial, US), rabbit anti-phospho histoneH3 (1:200, Merck Millipore), and rabbit anti-ki67 (1:200, Thermo Fisher Scientific). They were then incubated for 1 h with secondary antibodies: Alexa Fluor® 555 anti-guinea pig or anti-rabbit (1:500), Alexa Fluor® 488 anti-rabbit (1:250) (Thermo Fisher Scientific), and Cy2 anti-chicken (1:250, Jackson Immunoresearch, Suffolk, UK). Nuclei were stained with Hoechst 33258 (Sigma–Aldrich). Fluorescent images were captured using a Leica DMI 6000 B widefield microscope or a Leica TCS SPE confocal microscope. For morphometric analysis, p0 pancreases were sectioned at 3 μm and distributed as serial sections onto sets of 5 slides, and at least 10 sections per animal (45 μm apart) were analyzed. For other ages, pancreases were cut into tail, body, and head portions sectioned at 3 μm. A total of 2–3 sections (>100 μm apart) per portion and animal were analyzed. For Ki67, pHH3, and TUNEL assay, 2500–3000 insulin + nuclei were counted. Morphometric analyses were performed using Image J software (http://rsb.info.nih.gov/ij/index.html).

2.7. Optical projection tomography

Isolated pancreases were fixed in 4% paraformaldehyde and divided into the splenic, gastric, and duodenal lobes [30]. At this point, all samples were randomized and blinded for further Optical projection tomography (OPT) processing, which was performed as previously described [30,31]. Sample processing for OPT measurements was performed as follows: pancreatic specimens were freeze-thawed to increase permeability, bleached (in DMSO, Methanol, and hydrogen peroxide, 1:2:3, respectively, Thermo Fisher Scientific) to reduce endogenous fluorescence, and stained with primary guinea pig anti-insulin (1:500 dilution, Dako) and secondary goat Alexa 594 anti-guinea pig (1:500 dilution, Molecular Probes) antibodies. Once stained, all samples were mounted in 1.5% Low-melting SeaPlaque™ Agarose (Lonza Bioscience, Basel, Switzerland), dehydrated in pure Methanol (Thermo Fischer Scientific), and optically cleared using a 1:2 dilution of benzyl alcohol and benzyl benzoate, respectively (Acros organics). OPT imaging of cleared samples was performed using a BiOPTonics SkyScanner 3001 (version 1.3.13 SkyScan, Belgium). Once all iso-tropic voxel-based images were collected, image data sets were identically processed using a contrast limited adaptive histogram equalization (CLAHE), and post-acquisition misalignment correction was performed using Discrete Fourier Transform Alignment (DFTA). The processed and aligned frontal projection images were then reconstructed to tomographic sections (NRecon version 1.6.9.18, Bruker SkyScan) and uploaded to Imaris (version 8.1, Bitplane, UK). For insulin-positive volume quantifications, an iso-surface algorithm with a threshold value between 5 and 8 and a voxel filtering of 10 (corresponding to ≤50 μm diameter of a sphere) was applied to measure individual islet volumes and islet count.

2.8. cAMP measurements

Following the recovery culture, islets were incubated in Krebs solution containing 2.8 mM glucose for 1 h 30min at 37 °C with agitation. Then, batches of 20 islets were either resuspended immediately in 30 μl of lysis buffer (Cisbio assays, Parc Marcel Boiteux, France), supplemented with 0.5 mM IBMX (Sigma–Aldrich) for determination of basal cAMP levels or incubated for 20 min at 37 °C with IBMX (0.5 mM) and Forskolin (1 μM, Sigma–Aldrich) and then washed twice with HBSS-BSA and lysed as previously described. Lysates were kept at −80 °C until cAMP determinations using the cAMP dynamic 2 assay kit (Cisbio, Codolet, France).

2.9. Islet hormone content

Between 8 and 20 islets from p7, p14, and p28 mice were placed into an acid alcohol solution (75% ethanol, 0.18 N HCl), sonicated, and extracted overnight at 4 °C. The solution was then centrifuged to remove tissue in suspension and neutralized. Insulin and/or proinsulin concentrations were measured using mouse insulin and proinsulin ELISA kits (Mercodia).

2.10. Immunoblotting

Freshly isolated or cultured islets were lysed in triple detergent lysis buffer (Tris-HCl 50 mM, NaCl 150 mM, 0.1% SDS, 1% IGEPAL-CA630, 0.5% Sodium Deoxycholate, protease and phosphatase inhibitors), followed by sonication and frozen-thaw cycles. Protein concentration was measured with the Lowry protein assay kit (Bio-Rad, Hercules, CA, USA). Protein extracts (15–30 μg per replicate) were separated by SDS-PAGE electrophoresis onto 7.5–10% Tris-tricine gels and transferred to a Polyscreen PVDF membrane (Perkin Elmer, Waltham, MA, USA). Membranes were blocked for 1 h with TBS-0.05%Tween-5% BSA solution, followed by overnight incubation at 4 °C with the corresponding primary antibodies diluted in TBS.0.05%Tween: rabbit anti-MafA (1:250, Novus Biologicals), rabbit anti-p-Creb (S133), anti-Creb, anti-p-Erk1/2 (T202,Y204), anti-Erk, anti-p-Akt (T308), anti-Akt, anti-p-S6 (S235,S236), anti-S6 (1:1000, Cell Signaling Technology), and mouse anti-α-tubulin (1:1000; Sigma–Aldrich) as a loading control. Blots were visualized with ECL Reagent (Pierce Biotechnology,

Rockford, USA) using a LAS4000 Lumi-Imager (Fuji Photo Fil, Valhalla, NY). Protein spots were quantified with Image Studio Lite V5.2 software.

2.11. Dissociated isolated β cells and proliferation assay

After isolation and in order to eliminate fibroblasts, islets were cultured for 7 days in RPMI-1640 medium (Sigma—Aldrich) with 11 mM glucose, 10% FBS (Biosera), 2 mM L-glutamine, and antibiotics. Dissociated islet cells were obtained by treatment with 0.05% trypsin-EDTA for 4—5 min, seeded onto 384-well plates (15,000 cells/well), and cultured for 24 h with RPMI-1640 media supplemented as before. For proliferation assays, DICs were blanked overnight with RPMI-1640 medium containing 8 mM glucose and 0.1% FBS and then incubated for an additional 24 h period in the same media supplemented with the following reagents: exendin (200 nM), recombinant human Igf1 (10 nM), and recombinant human insulin (10 nM). During the last 5 h of culture, 5-Bromo-2′-deoxyuridine (5-BrdU) was added, and BrdU incorporation was determined using the Cell Proliferation ELISA kit (colorimetric) following the manufacturer's instructions (Roche Diagnostics, Mannheim, Germany).

2.12. Statistics

Data are presented as mean ± standard error of the mean (SEM). Statistical significance was tested using unpaired Student's t-test or two-way ANOVA for *in vivo* metabolic tests.

3. RESULTS

3.1. β-Cell specific Gsα knockout mice exhibit whole-body glucose intolerance

We generated mice in which the gene *Gnas* was ablated from β cells using *Ins1*^{Cre} knock-in mice (β-GsαKO, hereafter). Initially, to specifically evaluate the extent of Cre-mediated recombination, we introduced the reporter *R26-YFP* allele. Immunostaining against YFP revealed that most β cells had recombined this allele by postnatal day 28 (p28; Figure 1A). Next, to determine the extent of Gsα downregulation, we compared the expression of Gsα-coding transcripts in RNA that were isolated from whole islets and purified YFP^{+} cells of p28 β-GsαKO mice and their Cre-negative littermates. *Gnas* mRNA levels were reduced in knockouts compared to controls (about 50% and 90% in p28 islets and sorted p28 YFP^{+} cells, respectively; Figure 1B). The smaller reduction observed in islets compared to purified YFP^{+} cells is possibly due to non-recombined β-cells and/or non-β-cells present in the islets.

Next, we characterized whole-body glucose homeostasis in β-GsαKO mice. As a preliminary experiment, we confirmed that *Ins1*$^{Cre/+}$ knock-in mice did not show changes in whole-body glucose tolerance or insulin sensitivity compared to their wild-type littermates (Figure S1). Hence, Cre-negative littermates served as controls throughout the rest of the study. β-GsαKO mice had similar body weight as controls from p0 to p28 but weighed 20% less at 8 weeks of age (wo; Figure 1C). Random blood glucose levels were significantly higher in β-GsαKO mice than their control littermates from p14, with differences ranging from +28% at p0 to +180% at p28/8wo (Figure 1D). At 8wo, β-GsαKO mice displayed marked whole-body glucose intolerance without detectable changes in insulin sensitivity as compared to littermate controls (Figure S2). Importantly, impaired intraperitoneal and oral glucose tolerance in the context of normal insulin sensitivity was evident as early as p28 (Figure 1E—G), revealing that defects in glucose homeostasis develop during the first weeks of postnatal life. Glucose intolerance was associated with insufficient insulin as indicated by blunted glucose-induced insulin secretion and lower random plasma insulin levels in p28 GαKO as compared to controls (Figure 1H,I). In summary, β-GsαKO mice phenocopied the β-cell specific GsαKO mice generated with the *RIP2*-Cre transgene in terms of development of insulin-deficient diabetes. However, β-GsαKO mice did not exhibit the increased early postnatal lethality, linear growth retardation, or improved insulin sensitivity reported in the former model [21].

3.2. Deletion of Gsα in β cells results in limited postnatal β-cell mass expansion

We performed a histomorphometric analysis of the insulin-positive area in fixed pancreatic tissue from newborn to adult β-GsαKO mice and control littermates. β-GsαKO mice presented normal fractional β-cell areas at p0, indicating that the absence of Gsα does not impair β-cell formation during embryonic development (Figure 2A,B). At p14 we observed a tendency of decreased fractional β-cell areas (−28%), which became significant at p28 (Figure 2A,B). In agreement, β-cell mass was lower in p28 knockout relative to control animals (−25%), this difference becoming larger at 8wo (−50%; Figure 2C). By contrast, the α-cell mass was comparable between knockout and control mice from p14 to adulthood (Figure 2D). Using OPT [32], we identified an overall decrease in the islet number (−11%) and a specific reduction in islet volume corresponding to small islets ($<10^6$ um^3) in p28 β-GsαKO as compared to controls (Figure S3). Together, these results demonstrate that a loss of Gsα decreases β-cell mass. Furthermore, this effect first appears during the second to fourth weeks of life, supporting a role of Gsα-dependent signaling in postnatal β-cell mass establishment.

To define the cause of reduced postnatal β-cell growth, we studied β-cell proliferation and death. We found fewer proliferating β cells in p28 β-GsαKO pancreases than in controls, both using ki67 and phospho-Histone 3 immunostaining (Figure 2E,F). The number of double positive Insulin+/p-Histone3+ cells was already decreased at p14, indicating that β-cells from lactating β-GsαKO pups underwent mitosis at a lower rate than control β-cells. Compatible with decreased proliferation, gene expression analysis of cell cycle machinery genes revealed the downregulation of *Ccna2* and *Cdk4* and the upregulation of the inhibitor *Cdkn1a* (Figure 2G). Lastly, we examined whether the loss of Gsα was deleterious for β-cell survival but did not detect β-cell death by TUNEL assay at p14 or p28 in β-GsαKO or control pancreases (data not shown). Accordingly, apoptosis and endoplasmic reticulum stress genes were expressed at similar levels in animals from both genotypes (Figure S4). Therefore, the loss of Gsα impairs postnatal β-cell expansion through decreased β-cell proliferation, ostensibly without changes in β-cell survival.

3.3. Deletion of Gsα in β cells impairs postnatal β-cell maturation

During early postnatal life, β cells not only expand in number but also acquire functional maturity [33]. To determine the extent to which the absence of Gsα affects this latter process, we surveyed the expression of functionally relevant genes in p28 β-GsαKO islets. We found that the gene coding for the prohormone convertases Pcsk1 and Pcsk2 as well as genes typically upregulated during β-cell maturation, such as the exocytosis regulator Syt4 [34] and the mature β-cell marker Ucn3 [6], were decreased in β-GsαKO islets. Conversely, other genes expressed in β cells, such as *Iapp*, *Slc2a2*, *Gck,* or *Syt7* or the hormones genes *Gcg* (α-cell) and *Sst* (δ-cell), remained unchanged (Figure 3A), opposing the possibility that gene expression differences between β-GsαKO and control islets were merely due to variations in the portion of β cells. Among the transcription factors known to drive β-cell maturation, *NeuroD1* and *Nkx6.1* mRNAs levels were similar, *Pdx1* mRNA showed a tendency to be reduced ($p = 0.08$), and *Mafa* transcripts were significantly downregulated in β-GsαKO relative to control islets

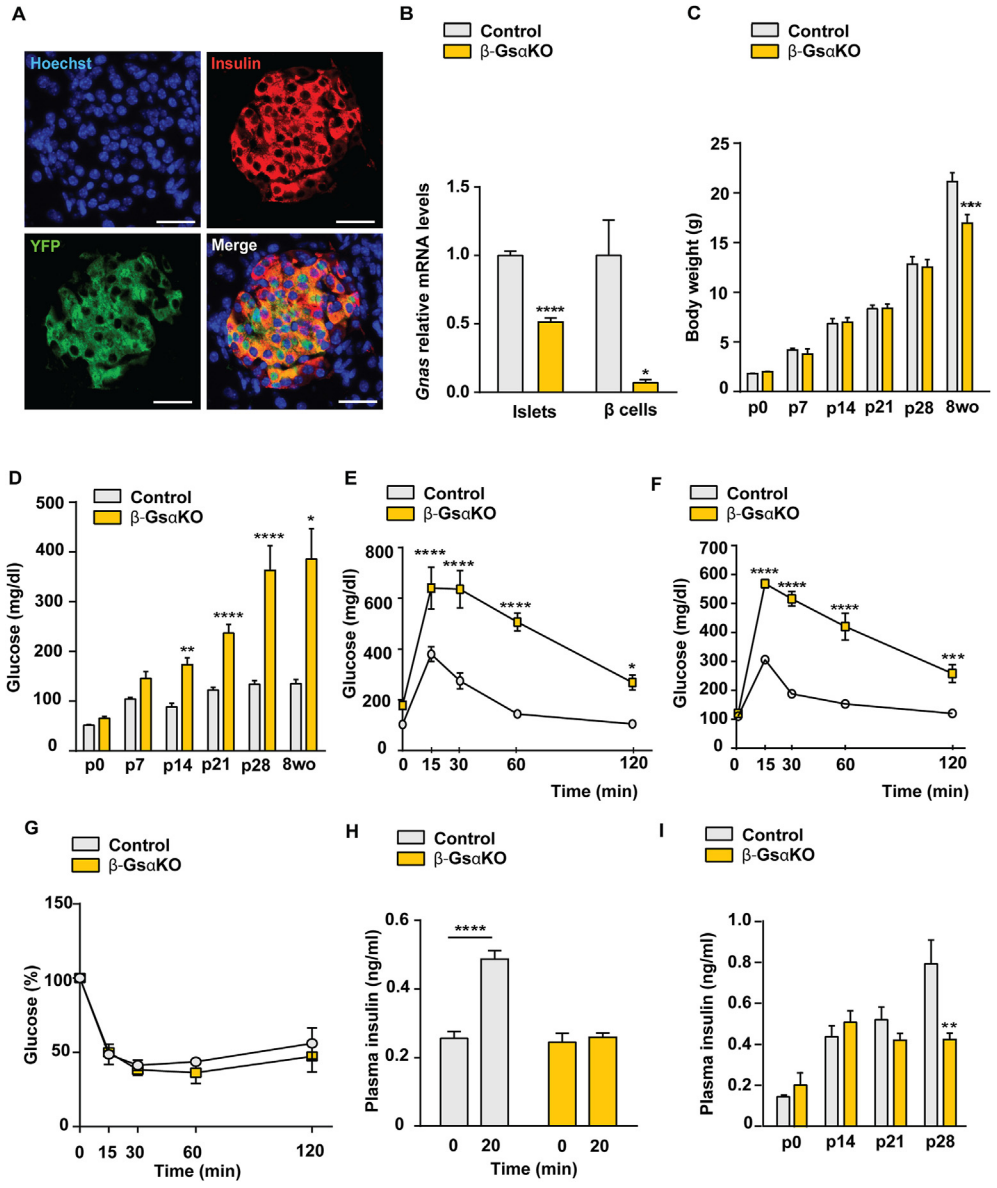

Figure 1: Whole-body glucose homeostasis in β-GsαKO mice. (A) Immunofluorescence staining of fixed pancreatic sections from p28 β-GsαKO/YFP mice using antibodies for insulin in red and YFP in green. Nuclei in blue were stained with Hoechst. Scale bars are 25 μm. **(B)** Quantification of *Gnas* mRNA levels by qPCR in islets and sorted β cells from p28 β-GsαKO (islets: n = 9; β cells: n = 6) and littermate controls (islets: n = 9; β cells: n = 5). Expression was normalized with *Tbp* and expressed relative to control, given the value of 1. **(C)** Body weight of β-GsαKO (n = 6) and control littermates (n = 6–10) at the indicated ages. **(D)** Non-fasting blood glucose of β-GsαKO (n = 4–7) and control littermates (n = 6–10) at the indicated ages**. (E,F)** Glucose tolerance tests were performed on 6 h fasted p28 β-GsαKO (n = 5) and control (n = 5–7) mice. A glucose load was administered via intraperitoneal injection **(E)** or by oral gavage **(F),** and blood samples were taken at the indicated times. **(G)** Insulin tolerance test of p28 β-GsαKO (n = 3) and control littermates (n = 3). **(H)** Plasma insulin levels before and 20 min after an intraperitoneal glucose injection in 6 h fasted p28 β-GsαKO (n = 5) and control (n = 5) mice. **(I)** Non-fasting plasma insulin of β-GsαKO (n = 7–13) and control littermates (n = 11–13) at the indicated ages. All bars and data points represent the mean ± SEM. $*P < 0.05$, $**P < 0.01$, $***P < 0.001$, $****P < 0.0001$ *vs.* control animals (B-G, I) or between time points (H) using two-tailed Student's test (B,H) and two-way ANOVA (C-G, I).

(Figure 3A). In agreement, Mafa protein was reduced in p28 β-GsαKO mice as assessed by immunoblot analysis using whole islet extracts and immunofluorescence staining in fixed pancreatic tissue (Figure S5). Examining *Mafa* and *Pdx1* mRNA levels at an earlier time revealed that both genes were downregulated at p7 (Figure 3B), demonstrating an early requirement of Gsα-dependent signaling for the expression of these two transcription factors in young postnatal β cells. Finally, we checked the expression of several mRNAs normally repressed in mature β cells, including the transcription factors *Neurog3*, *Sox9*, and *Mafb* and the enzymes *Hk1*, *Ldha*, *Cat*, and *Oat*, which belong to the designated β-cell disallowed genes. All these genes were expressed at comparable low levels in p28 β-GsαKO and control islets (Figure S6), thus indicating that β cells in β-GsαKO mice do not exhibit a progenitor-like state.

β-GsαKO islets also displayed reduced insulin content as measured by ELISA, ranging from 52% to 8% of controls at p7 and 8wo, respectively (Figure 3C). Magnification of the difference was mainly due to the absence of an age-dependent increase in the total islet insulin content in β-GsαKO islets relative to controls (Figure 3C). Weaker insulin immunostaining in β-GsαKO islets, compared to size-matched control

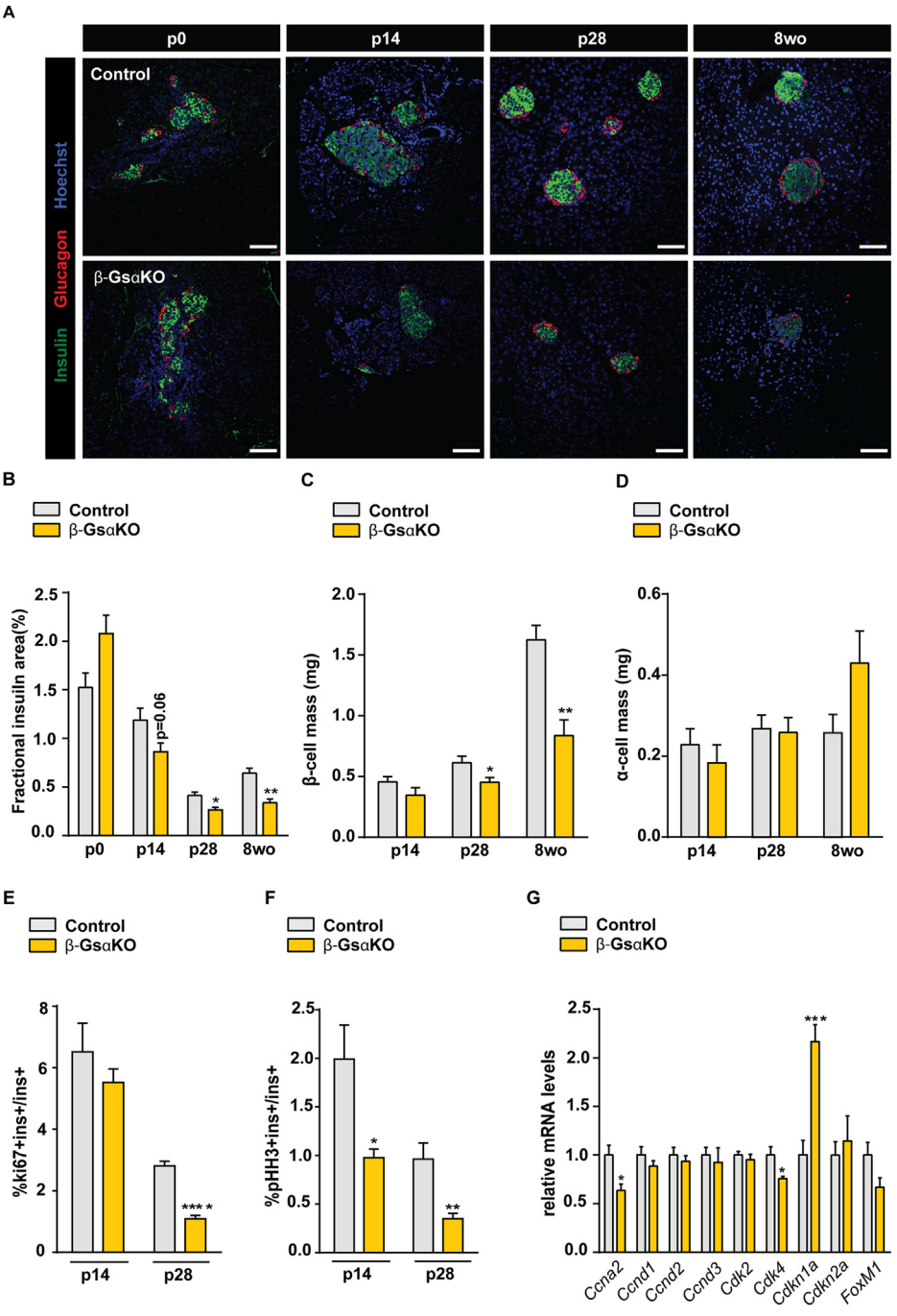

Figure 2: Characterization of the β-cell compartment in β-GsαKO mice. (A) Representative immunofluorescence images of fixed pancreatic sections from control and β-GsαKO mice at the indicated ages, stained for insulin in green and glucagon in red. Nuclei are marked with Hoechst in blue. Scale bars are 75 μm. **(B)** Fractional insulin area was calculated as the percentage of insulin+ area relative to the total pancreatic area (p0: n = 4, p14/p28: n = 5, 8wo: n = 3). **(C,D)** Quantification of β-cell **(C)** and α-cell **(D)** mass. Values were calculated by multiplying fractional insulin area x pancreas weight (p14/p28: n = 5, 8wo: n = 3–4). **(E,F)** Quantification of the percentage of β (insulin+) cells that are Ki67+ **(E)** or p-HH3+ **(F)** in pancreases from p14 and p28 β-GsαKO (n = 5) and control (n = 4) mice**. (G)** Quantification of the expression of the indicated cell cycle and proliferation genes in p28 β-GsαKO (n = 4–10) and control (n = 4–9) islets as determined by qPCR. Expression was normalized with *Tbp* and expressed relative to control, given the value of 1. All bars represent the mean ± SEM. $^{*}P < 0.05$, $^{**}P < 0.01$, $^{***}P < 0.001$, $^{****}P < 0.0001$ vs. control animals by two-tailed Student's test.

islets, suggest decreased insulin protein content per cell (Figure 3D). Mafa and Pdx1 are transcriptional regulators of the *Insulin* gene, and therefore, we postulated that decreased *Ins* gene transcription might be responsible for reduced islet insulin content in knockout islets. We found that *Ins1* mRNA levels were reduced by ~50% (conceivably due to the inactivation of one *Ins1* allele in *Ins1*$^{Cre/+}$ knock-in mice), whereas the *Ins2* gene expression was unaltered at both p7 and p28 (Figure 3E). However, because *Ins1* is expressed much less than *Ins2* in β cells [35], this gene is not considered the primary determinant for insulin production. Therefore, translational and/or post-translational

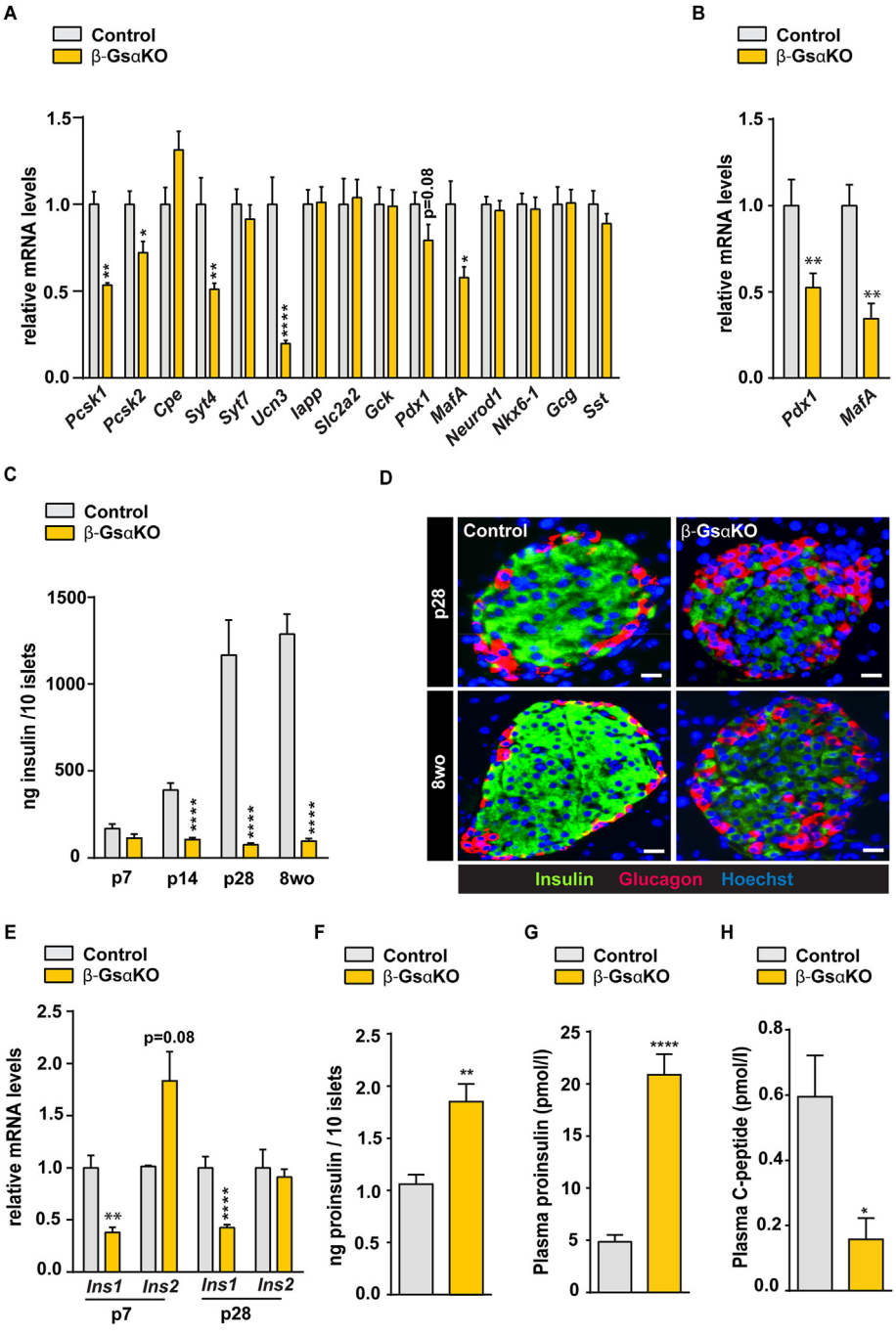

Figure 3: β-cell maturation in β-GsαKO mice. (A) Quantification of the expression of the indicated genes by qPCR in p28 β-GsαKO (n = 4–15) and control (n = 4–13) islets. Expression was normalized with *Tbp* and expressed relative to control, given the value of 1. **(B)** *Pdx1* and *Mafa* mRNA levels in p7 β-GsαKO (n = 5–6) and control (n = 6) measured by qPCR. Expression was normalized with *Tbp* and expressed relative to control, given the value of 1. **(C)** Insulin content of β-GsαKO and control islets isolated at the indicated ages and determined by ELISA (p7, n = 4–5; p14, n = 11; p28, n = 8–14; 8wo, n = 28–32). **(D)** Representative immunofluorescence images of islets matched for size from β-GsαKO and control mice. Insulin is shown in green, glucagon in red, and nuclei in blue. Images were taken using the same exposure times for comparison purposes. Scale bars are 10 μm. **(E)** Quantification of the expression of the *Ins1* and *Ins2* genes by qPCR in β-GsαKO and control islets at p7 (n = 3–6) and p28 (n = 6–8). Expression was normalized with *Tbp* and expressed relative to control, given the value of 1. **(F)** Proinsulin content of p28 β-GsαKO (n = 4) and control (n = 7) islets as determined by ELISA. **(G)** Plasma proinsulin levels in p28 β-GsαKO (n = 6) and control (n = 8) mice. **(H)** Plasma C-peptide levels in p28 β-GsαKO (n = 4) and control (n = 4) mice. All bars represent the mean ± SEM. $*P < 0.05$, $**P < 0.01$, $***P < 0.001$, $****P < 0.0001$ vs. controls by two-tailed Student's test.

mechanisms are likely involved in reduced insulin islet content in knockout islets. We postulated that reduced processing of proinsulin into mature insulin might contribute to the diminished islet insulin content, as the genes encoding the processing enzymes Pcsk1 and Pcsk2 were downregulated in knockout islets (Figure 3A). In line with this idea, proinsulin content was 1.8-fold higher in β-GsαKO islets relative to controls (Figure 3F). This difference in proinsulin content translated into a 4.2-fold increase in circulating proinsulin levels and a

72% reduction of circulating levels of C-peptide in p28 β-GsαKO mice (Figure 3G,H).

Collectively, these observations indicate that Gsα-dependent signaling is involved in the acquisition of β-cell maturity during postnatal stages.

3.4. Loss of Gsα reduces intracellular cAMP and Creb-dependent signaling in postnatal islets

As an initial step to gain insight into the molecular mechanisms responsible for reduced functional β-cell mass in β-GsαKO mice, we studied intracellular cAMP levels in isolated islets from p28 and 8 wo mice. At both ages and under basal conditions, β-GsαKO islets presented cAMP levels of approximately 15% of controls of the same age (Figure 4A). Further, despite the combination of the adenylyl cyclase activator forskolin and the phosphodieserase inhibitor IBMX elevating cAMP levels by 4-fold and 12-fold in p28 and 8 wo β-GsαKO islets respectively, the cAMP content remained much lower than in stimulated controls (8 and 14% of controls at p28 and 8wo, respectively; Figure 4A). These results show that loss of Gsα severely depletes intracellular cAMP levels, jeopardizing cAMP-dependent signaling in islets.

Protein kinase A (PKA) is considered one of the primary mediators of cAMP signaling in the cell. We surveyed gene expression of components of the PKA branch and found that mRNAs for the regulatory and catalytic subunits of PKA, *Prkar1b* and *Prkaca,* as well as the anchor protein *Akap11* were reduced in knockout islets as compared to controls (Figure 4B). Likewise, the expression of the *Creb3* gene encoding the cAMP response element binding (Creb) transcription factor, a main downstream effector of PKA signaling, was also decreased. To validate these results, we studied Creb at the protein

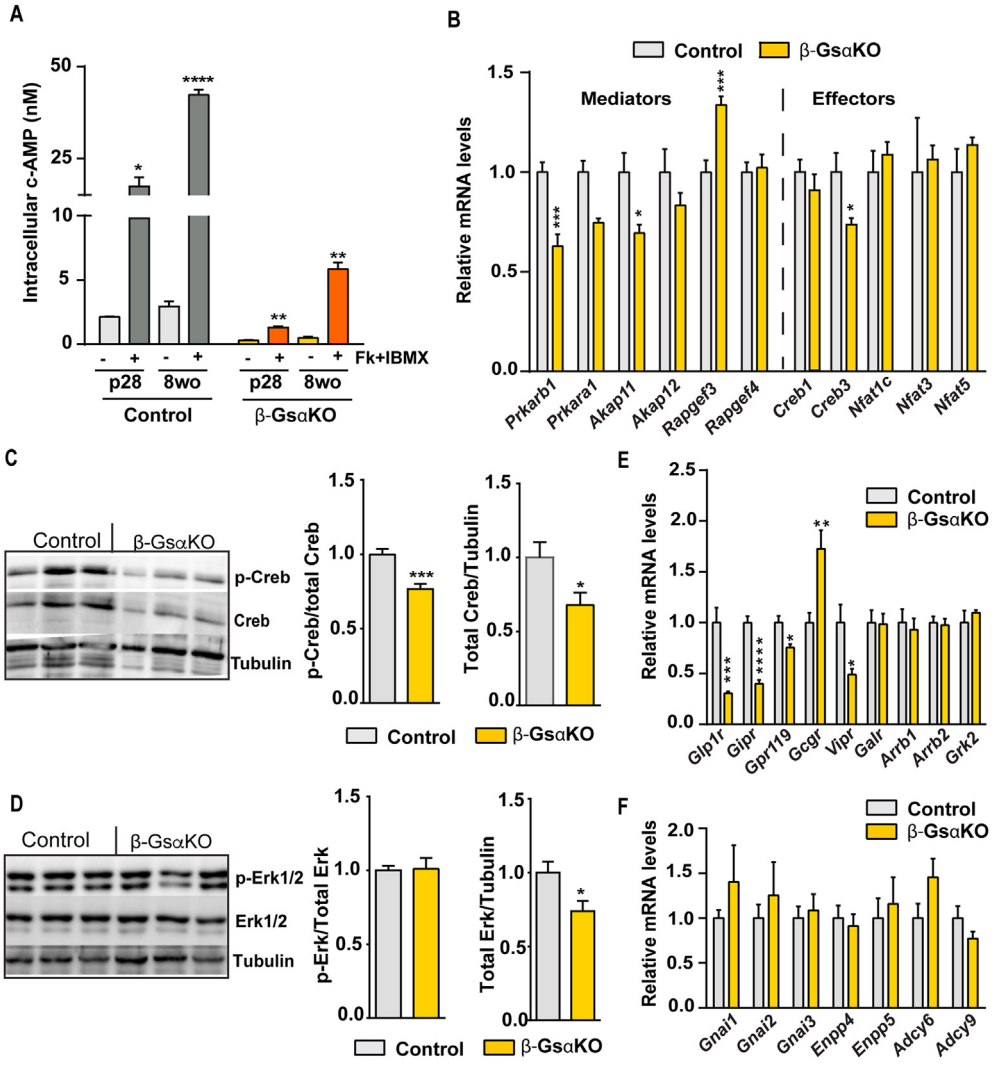

Figure 4: cAMP signaling pathway in β-GsαKO islets. (A) Intracellular cAMP concentration in freshly isolated p28 and 8wo β-GsαKO and control islets incubated for 20 min with or without forskolin (1 μM) + IBMX (0.5 mM) (n = 3). **(B)** Expression of the indicated genes in p28 β-GsαKO (n = 4–8) and control (n = 4–9) islets as determined by qPCR. Expression was normalized with *Tbp* and expressed relative to control, given the value of 1. **(C)** Determination of phospho(p)-Creb and total Creb by immunoblot analysis in the whole islet extract from p28 β-GsαKO and control islets. Left: representative immunoblot image. Right: quantification of p-Creb (relative to total Creb) and Creb (relative to tubulin) levels. Values are expressed relative to control islets, given the value of 1 (n = 7–10). **(D)** Determination of phospho(p)-Erk1/2 and total Erk1/2 by immunoblot analysis in whole islet extracts from p28 β-GsαKO and control islets. Left: representative immunoblot image. Right: quantification of Erk1/2 activation (p-Erk1/2/total Erk1/2). Values are expressed relative to control islets, given the value of 1 (n = 7). **(E,F)** Quantification of the indicated genes by qPCR in p28 β-GsαKO (n = 4–8) and control (n = 4–9) islets. Expression was normalized with *Tbp* and expressed relative to control, given the value of 1. All data points represent the mean ± SEM. $*P < 0.05$, $**P < 0.01$, $***P < 0.001$, $****P < 0.0001$ vs. controls by two-tailed Student's test.

level. At p28, β-GsαKO islets contained less Creb protein and displayed lower Creb phosphorylation (relative to total Creb) than controls (Figure 4C). Our prior results showing downregulation of *Ccna2*, *Mafa,* and *Pcsk1* in p28 β-GsαKO islets (see Figures 2G and 3A) reinforce this finding, as these genes have been reported to be direct Creb targets [15,36,37]. Therefore, these results support the reduction of PKA/Creb signaling in p28 β-GsαKO islets.

In addition to PKA, cAMP can trigger signaling through guanine nucleotide exchange proteins, directly activated by cAMP (Rapgef; formally known as Epac factors) [38], which can then regulate gene expression via the Calcineurin/Nuclear factor of activated T-cells (Nfat), a factor family of transcriptional regulators [39]. Importantly, Nfat signaling has been shown to regulate postnatal β cell development [40]. Among the *Rapgef* and *Nfat* genes expressed in islets, only *Ragef3* gene expression was changed (30% increase) in β-GsαKO as compared to controls (Figure 4B). In islets, ePAC/Rap1 regulates the MAP kinases Erk1/2 [41], which have been reported to phosphorylate Creb [42] and induce β-cell proliferation [43]. Similar to Creb, total Erk1/2 protein was modestly decreased in β-GsαKO islets (Figure 4D). However, the degree of Erk1/2 activation was similar in knockout and control islets (Figure 4D). Together, these results indicate that signaling through the ePAC branch is not grossly impacted by Gsα loss in p28 islets.

Next, we investigated whether loss of Gsα had effects on the expression of other proximal components of the cAMP signaling machinery. Of the GPCR-Gs receptors tested, we found that the incretin receptors *Glp1r* and *Gipr*, the cannabinoid receptor *Gpr119*, and the PAPAC/VIP receptor *Vipr* were significantly downregulated in β-GsαKO as compared to control islets, whereas the glucagon receptor (*Gcgr*) was upregulated (Figure 4E). By contrast, gene expression of GPCR desensitizers, including β-arrestins (*Barr1*, *Barr2*) or G protein-coupled receptor kinases (*Grk2*), was unaltered in p28 β-GsαKO islets (Figure 4E). Lastly, we assessed whether Gsα inactivation exerted compensatory effects on the expression of other genes involved in regulating cAMP levels, including the mechanistically opposed G protein subclass Gi, phosphodiesterases, and adenylyl cyclases. However, we found that all the genes assayed were similarly expressed in β-GsαKO and control islets (Figure 4F).

3.5. Loss of Gsα impairs insulin signaling in postnatal islets

Mouse models targeting one or more proteins in the insulin/insulin-like growth factor (Igf) transduction pathway show that this pathway regulates β-cell proliferation [44–47]. Expression of proximal components of this pathway, namely the Igf1 receptor (Igf1r) [20,48] and Insulin receptor substrate 2 (*Irs2*) [49], are known to be regulated by cAMP, indicating the possibility that impaired insulin/Igf signaling causes the β-cell mass phenotype of β-GsαKO mice. However, this hypothesis was rejected in *RIP2*-Cre/GsαKO mice due to the normality of the *Irs2* expression in adult islets from this model. Here, we reexamined this notion in more detail using islets at a younger age. First, we assessed the activation status of the main intracellular effector of the insulin/Igf1 pathway, the kinase Akt/PKB. We found that phosphorylated Akt (active state) was significantly reduced in p28 β-GsαKO relative to control islets (Figure 5A), confirming that the loss of Gsα negatively affects insulin-signaling activity in postnatal β cells. We then measured the phosphorylation of ribosomal protein S6, which is activated downstream of Akt and required for Akt-driven β-cell proliferation [50], and found that it was decreased in β-GsαKO islets (Figure 5B), linking anomalies in this pathway to the postnatal β-cell expansion defect in β-GsαKO mice.

To reveal the molecular alterations responsible for abnormal insulin/Igf signaling activity, we first examined the expression of the cAMP/Creb target *Irs2* in islets from p28 β-GsαKO mice. We found that, in agreement with the earlier study in the *RIP2*-Cre/GsαKO model, the *Irs2* gene expression was unaltered (Figure 5C). As Irs2 is expressed in all cell types of the islet [51], we also assayed its expression in sorted β cells and found that it was significantly downregulated in knockout β cells compared to controls (Figure 5C). Though this result confirms that *Irs2* is a target of Gsα signaling in β cells, β-cell specific inactivation of *Irs2* had no impact on β-cell mass in the early postnatal period [46]. Thus, alterations in Irs2 alone cannot explain the β-cell expansion defect in β-GsαKO mice.

cAMP also regulates the expression of the Igf1r receptor (Igf1r) in islets [20,48]. Though genetic ablation of *Igf1r* has no impact on β-cell mass [52], β-cell specific compound deletion of *Igf1r* and the insulin receptor *(Insr)* was reported to reduce β-cell mass as early as p14 [44]. This body of knowledge prompted us to look at the status of both receptors in β-GsαKO mice. Using immunoblot analysis, we found that Igf1r and Insr protein levels were decreased in p28 β-GsαKO islets (Figure 5D). In contrast, though *Igf1r* gene expression was downregulated, *Insr* mRNA levels were similar in p28 β-GsαKO islets and controls (Figure 5E), suggesting that different mechanisms cause the depletion of these receptors in β-GsαKO islets. The Insr has two isoforms (i.e., Insr-A and Insr-B), derived from alternative splicing of the same *pre-Insr* mRNA. We performed conventional RT-PCR using primers of exons 10 and 12, which permit amplification of the two splice variants. As shown in Figure 5F, we observed that β-GsαKO islets presented a higher InsrA:InsrB ratio. Using qPCR, we quantified *Insr*-B (including exon 11) transcripts and found that they were significantly reduced at p28, using both islet and sorted β cells RNA (Figure 5G), confirming that the loss of Gsα specifically affects the expression of the Insr-B isoform within β cells. The InsrA:InsrB ratio is regulated by several splicing factors, some of which promote inclusion (i.e., Srsf1, Srsf3, Mbln1), whereas others promote exclusion (Celf1) of exon 11 [53]. The relative expression of these factors determines the degree of exon 11 inclusion and thereby Insr isoform distribution. Nicely correlating with reduced *Insr-B* mRNA levels, we found that p28 β-GsαKO islets exhibited decreased *Srsf1* and increased *Celf1* expression (Figure 5H). Together, these findings reveal that Gsα signaling not only regulates Igf1r but also Insr in β cells. Importantly, the downregulation of *Igf1r* and *Insr-B* was evident as early as p7 (Figure 5I), placing defective signaling through these receptors at the correct time to negatively impact postnatal β-cell mass expansion in β-GsαKO mice.

Finally, we measured BrdU incorporation in dissociated islet cells (DICs) from p28 β-GsαKO and control islets following incubation with insulin, Igf1, and the Glp1 agonist Exendin as control. While control DICs augmented BrdU incorporation in response to the three molecules, β-GsαKO DICs only responded to Igf1 (Figure 5J). Therefore, Gsα ablation impairs the proliferative activity of insulin in postnatal islets, indicating that deficient insulin signaling contributes to the β-cell mass phenotype in β-GsαKO mice.

4. DISCUSSION

In mice, pancreatic β-cell development culminates in two essential milestones during the first weeks of postnatal life. First, the proliferation of neonatal β cells leads to the rapid expansion of the β-cell mass. Second, β cells acquire the ability to secrete appropriate amounts of insulin in response to glucose. Here we demonstrate that the specific disruption of Gsα signaling in β cells compromises both processes, resulting in an inadequate functional β-cell mass that cannot maintain proper glucose homeostasis in adult life. Importantly, these changes occur in the absence of other alterations described in

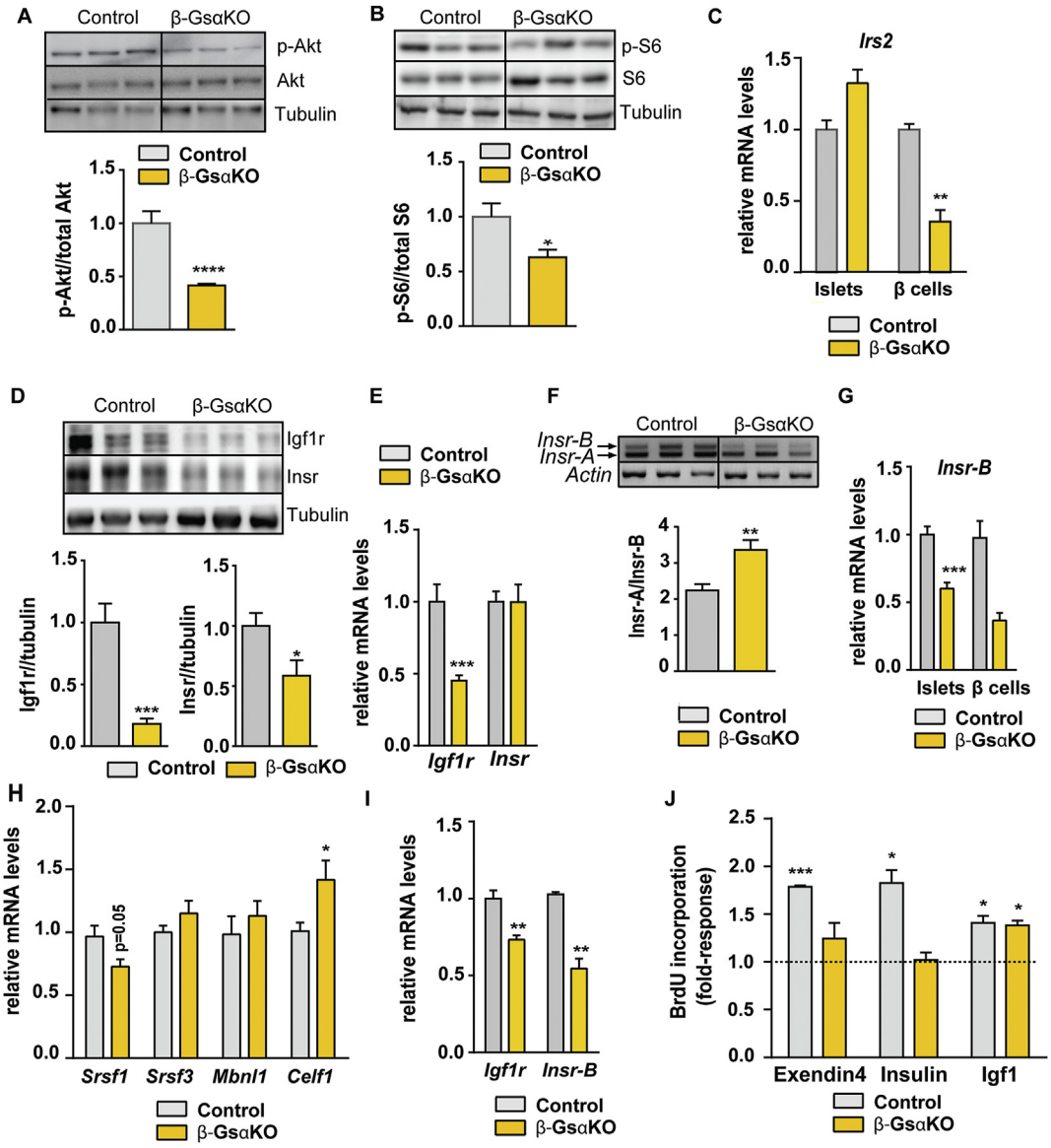

Figure 5: Insulin signaling in β-GsαKO islets. (A) Determination of phospho(p)-Akt and total Akt by immunoblot analysis in whole islet extracts from p28 β-GsαKO and control mice. Top: representative immunoblot image. Bottom: quantification of Akt activation (p-Akt/2/total Akt) (n = 12). Values are expressed relative to control islets, given the value of 1. **(B)** Determination of phospho(p)-S6 and total S6 by immunoblot analysis in whole islet extracts from p28 β-GsαKO and control mice. Top: representative immunoblot image. Bottom: quantification of S6 activation (p-S6/total S6) (n = 6–7). Values are expressed relative to control islets, given the value of 1. **(C)** Quantification of *Irs2* mRNA levels by qPCR in islets (n = 9–10) and sorted β cells (n = 3–5) from p28 β-GsαKO and littermate controls. Expression was normalized with *Tbp* and expressed relative to control, given the value of 1. **(D)** Determination of Igf1r and Insr protein levels by immunoblot analysis in whole islet extracts from p28 β-GsαKO and control mice. Top: representative immunoblot image. Bottom: quantification of Igf1r and Insr protein levels relative to tubulin (n = 8). Values are expressed relative to control islets, given the value of 1. **(E)** Quantification of *Igf1r* and total *Insr* mRNA levels by qPCR in p28 β-GsαKO and control islets (n = 8–9). Expression was normalized with *Tbp* and expressed relative to control, given the value of 1. **(F)** Gene expression of Insr-A and Insr-B isoforms in p28 β-GsαKO and control islets as determined by conventional PCR. Top: representative gel. Bottom: quantification of the ratio Insr-A/Insr-B (n = 6). *Actin* is shown as a housekeeping gene. **(G)** Quantification of *Insr*-B mRNA levels by qPCR in islets (n = 4–6) and sorted β cells (n = 2) from p28 β-GsαKO and control mice. Expression was normalized with *Tbp* and expressed relative to control, given the value of 1. **(H)** Expression of genes encoding factors involved in Insr splicing in p28 β-GsαKO (n = 5–8) and control (n = 3–8) islets as determined by qPCR. Expression was normalized with *Tbp* and expressed relative to control, given the value of 1. **(I)** *Igf1r* and *Insr-B* mRNA levels in p7 β-GsαKO (n = 5–9) and control (n = 3–6) measured by qPCR. Expression was normalized with *Tbp* and expressed relative to control, given the value of 1. **(J)** Proliferation determined by BrdU incorporation in DICS prepared from 5 wo β-GsαKO and control islets, and stimulated for 24 h with exendin-4 (200 nM), insulin (11 nM) or Igf1 (11 nM) (n = 3, with 6 replicates per experiment). Values are expressed as fold-increase over un-stimulated DICS. All data points represent the mean ± SEM. $P < 0.05$, $^{**}P < 0.01$, $^{***}P < 0.001$ vs. control animals by two-tailed Student's test.

RIP2-Cre/GsαKO mice [21], including poor postnatal growth, reduced survival, or enhanced *in vivo* insulin sensitivity, indicating that off-target Cre-mediated recombination events likely caused these effects [24] in the former model.

The identity of the endogenous ligands and GPCRs that function via Gsα to regulate postnatal β-cell development remains poorly explored. Here, we show that β-GsαKO islets present decreased expression of some Gsα-GPCRs, including the receptors for the incretin hormones

Glp1 and Gip, the receptor for PACAP/VIP and the orphan receptor Gpr119, all of which have been shown to potentiate glucose-induced insulin secretion and hence regulate β-cell function. Incretins, especially Glp1, are also inducers of β-cell proliferation and could therefore be potentially involved in the defects in postnatal β-cell growth of β-GsαKO mice. However, mouse models of disrupted incretin receptor action lack alterations in β-cell mass establishment under homeostatic conditions [54–57], challenging the idea that defective incretin signaling underlies the defects in postnatal β-cell growth observed in β-GsαKO mice. Likewise, the absence of β-cell mass phenotypes after the genetic disruption of *Grp119* or *Vip* in mice challenges the dominant roles of these two molecules in postnatal β-cell expansion [58,59]. Multiple other Gsα-GPCRs exist, some of which have been described in young β cells [22]. It will be interesting to study if they are affected in β-GsαKO mice and involved in the β-cell growth defect observed in this model. An alternative view is that the β-cell defects observed in β-GsαKO mice do not derive from anomalies in individual ligands or receptors, but rather, they are a consequence of the complete blockade of Gαs-GPCRs signaling and the resulting loss of counteregulation of Giα-GPCRs signaling, which is known to limit β-cell expansion during the perinatal period [22].

In eukaryotic cells, two primary intracellular mediators, the kinase PKA and the exchange factors Epac, control the cellular functions of cAMP [38]. Our results indicate that the inactivation of Gsα impairs PKA signaling, as illustrated by the reduced activation of its principal effector, the transcription factor Creb. In accordance, several genes reported to be regulated by Creb activity and involved in β-cell proliferation (i.e., *Ccna2*, *cdkn1a*) and maturation (i.e., Pdx1 and Mafa) were downregulated in β-GsαKO islets [13–15,35,36], directly connecting Gsα/PKA/CREB signaling to postnatal β-cell development. Interestingly, Mafa disruption has been shown to reduce β-cell proliferation and alter β-cell gene expression by 3 weeks of age [60]. Moreover, some of the genes regulated by this transcription factor are decreased in p28 β-GsαKO islets (namely, *Pcsk1*, *Ucn3*, *Glp1r*) [60–62]. Collectively, this evidence supports the claim that aberrant Mafa induction contributes to impaired postnatal β-cell development in β-GsαKO mice.

The involvement of the Epac factors in abnormal β-cell development in β-GsαKO mice is less clear. Epac proteins are known to participate in exocytosis and influence the release of Ca2+ [10], which could potentially link Gsα/cAMP with the calcineurin/Nfat pathway [39], a well-known regulator of postnatal β-proliferation and maturation [40]. Interestingly, research demonstrates that the mitogenic effects of Glp1r activation in human islets require activation of the Nfat genes [63]. However, we found that neither *Epac* nor *Nfat* genes were modified in β-GsαKO islets. Likewise, genes found to be downregulated upon disruption of calcineurin/Nfat signaling, such as *Ins2*, *Gck*, *Slc2a2,* or *Iapp,* were unaffected, implying that Epac/Nfat proteins are unlikely to be the primary mediators of Gsα effects in early postnatal β cell development.

Our work shows that Gsα inactivation jeopardizes insulin signaling in postnatal β cells. Though the crosstalk between the Gsα/cAMP and insulin pathways has been previously recognized in adult β cells, this study reveals that this connection is present from early postnatal life. At p28, Gsα-depleted β cells exhibit a diminished expression of *Igf1r* and *Irs2*, two previously recognized cAMP/Creb targets [20,48,49]. Intriguingly, here we uncover a new interaction at the level of the insulin receptor that may expound upon the postnatal β-cell expansion defect of β-GsαKO mice. Indeed, the β-cell mass phenotype of β-GsαKO mice is reminiscent of the phenotype described in mice carrying a compound deletion of *Igf1r* and *Insr* in β cells, namely reduced postnatal β-cell mass associated with decreased phosphorylated Akt and Mafa expression [44]. Of note, reduced β-cell mass was only observed in adult stages upon inactivation of *Insr* alone [45] or not observed at all upon a single deletion of *Igf1r* [52], suggesting that insulin might play a dominant role in postnatal β-cell growth. In this regard, it is significant that β-GsαKO islets exhibit severely depleted insulin content from shortly after birth. It may be argued that diminished autocrine insulin signaling (due to the combination of decreased insulin content and down-regulation of insulin signaling elements) underlies the β-cell expansion defect in β-GsαKO mice. We acknowledge that the autocrine actions of insulin are still a matter of debate [64,65]. However, most of the studies addressing this question have used adult β cells, and their intrinsic features and the microenvironment they reside in (i.e., proportion of other endocrine cells, islet vascularization, or innervation) are different from postnatal β cells. Thus, it is plausible that autocrine insulin signaling exerts discrepant roles in young and adult β cells.

The molecular mechanisms that connect Gsα with the insulin receptor remain to be further elucidated. The insulin receptor protein has two isoforms (A and B) generated by alternative splicing of the *Insr* gene (A: exon 11 excluded; B: exon 11 included) that differ in binding affinities and activation of downstream signaling pathways [66]. Moreover, the relative proportion of these isoforms is cell-specific and can vary during development and changing environmental conditions. Here, we show that loss of Gsα results in decreased levels of the *Insr-B* isoform in β cells. In agreement, gene expression of the splicing factor Srf1, which promotes exon 11 inclusion, is reduced, though the gene expression of the factor Celf1, which causes exon 11 skipping, is increased in β-GsαKO islets. Remarkably, insulin induces the generation of Insr-B in islets [67]. Therefore, reduced Insr-B levels could be a consequence of impaired insulin signaling activity. In support of this possibility, the splicing factor Srsf1 has also been reported to enhance Insr exon 11 inclusion upon insulin stimulation in islets [67]. To date, the role of *Insr* alternative splicing and the importance of the different Insr isoforms for pancreatic β-cell proliferation, survival, or function is unclear. Interestingly, the Insr-B isoform is associated with stronger insulin binding and might play a role in β-cell survival [67]. It will be interesting to address how alternative splicing of the Insr regulates postnatal β-cell proliferation and/or maturation in the future.

Collectively, our study, using conditional ablation of Gsα in β cells, reveals critical functions of Gsα-dependent signaling in postnatal β cell expansion and maturation. We also show that inactivation of Gsα has an early and broad impact on several proximal elements of the insulin signaling transduction machinery and propose that these alterations are involved in impaired postnatal β cell development in β-GsαKO mice. Remarkably, we identify the insulin receptor as a target of Gsα-dependent signaling in postnatal β cells. This finding encourages further work to decipher whether this interaction is conserved in adult β cells and whether it could be exploited to expand or preserve adult β cell mass in diabetes.

AUTHOR CONTRIBUTION

BSN conducted all experiments. RFR and AG provided assistance with mouse experiments and proliferation assays. MPJ, EFR, JMC, and YE provided assistance in several experiments. JM and SD performed cAMP studies. MH and UA performed OPT studies. LSW provided floxed Gnas mice. RGo and RGa conceived the project. BSN, JV, RGo, and RGa analyzed and discussed the data. BSN and RGa wrote the manuscript. All authors read and approved the manuscript.

ACKNOWLEDGEMENTS

This work has been supported by projects PI16/00774 (RGa) and PI19/00896 (RGa and RGo) integrated in the Plan Estatal de I+D+I and cofinanced by ISCIII-Subdirección General de Evaluación and Fondo Europeo de Desarrollo Regional (FEDER-"A way to build Europe"); grant 2014 SGR659 from the Generalitat de Catalunya and Fundación DiabetesCero (RGa). The research leading to these results has received funding from the European Community's Seventh Framework Programme (FP7/2009–2013) under the grant agreement n°229673 (EFR). CIBERDEM (Centro de Investigación Biomédica en Red de Diabetes y Enfermedades Metabólicas Asociadas) is an initiative of the Instituto de Salud Carlos III.

CONFLICT OF INTEREST

None declared.

APPENDIX A. SUPPLEMENTARY DATA

Supplementary data to this article can be found online at https://doi.org/10.1016/j.molmet.2021.101264.

REFERENCES

[1] Butler, P.C., Meier, J.J., Butler, A.E., Bhushan, A., 2007. The replication of beta cells in normal physiology, in disease and for therapy. Nature Clinical Practice Endocrinology and Metabolism 3(11):758–768.

[2] Bouwens, L., Rooman, I., 2005. Regulation of pancreatic beta-cell mass. Physiological Reviews 85(4):1255–1270.

[3] Zeng, C., Mulas, F., Sui, Y., Guan, T., Miller, N., Tan, Y., et al., 2017. Pseudotemporal ordering of single cells reveals metabolic control of postnatal β cell proliferation. Diabetes 25(5):1160–1175 e1111.

[4] Wang, Y., Sun, J., Ni, Q., Nie, A., Gu, Y., 2019. Dual effect of raptor on neonatal β-cell proliferation and identity maintenance. Diabetes 68(10):1950–1964.

[5] Wang, P., Fiaschi-Taesch, N.M., Vasavada, R.C., Scott, D.K., Garcia-Ocana, A., Stewart, A.F., 2015. Diabetes mellitus–advances and challenges in human beta-cell proliferation. Nature Reviews Endocrinology 11(4):201–212.

[6] Blum, B., Hrvatin, S., Schuetz, C., Bonal, C., Rezania, A., Melton, D.A., 2012. Functional beta-cell maturation is marked by an increased glucose threshold and by expression of urocortin 3. Nature Biotechnology 30(3):261–264.

[7] Salinno, C., Cota, P., Bastidas-Ponce, A., Tarquis-Medina, M., Lickert, H., Bakhti, M., 2019. Beta-cell maturation and identity in health and disease. International Journal of Molecular Sciences 20(21).

[8] Yoshihara, E., Wei, Z., Lin, C.S., Fang, S., Ahmadian, M., Kida, Y., et al., 2016. ERRγ is required for the metabolic maturation of therapeutically functional glucose-responsive β cells. Cell Metabolism 23(4):622–634.

[9] Stolovich-Rain, M., Enk, J., Vikesa, J., Nielsen, F.C., Saada, A., Glaser, B., et al., 2015. Weaning triggers a maturation step of pancreatic β cells. Developmental Cell 32(5):535–545.

[10] Tengholm, A., Gylfe, E., Shibasaki, T., Takahashi, T., Takahashi, H., Seino, S., et al., 2017. cAMP signalling in insulin and glucagon secretion. Diabetes, Obesity and Metabolism 19(2):42–53.

[11] Seino, S., 2012. Cell signalling in insulin secretion: the molecular targets of ATP, cAMP and sulfonylurea. Diabetologia 55(8):2096–2108.

[12] Müller, T.D., Finan, B., Bloom, S.R., D'Alessio, D., Drucker, D.J., Flatt, P.R., et al., 2019. Glucagon-like peptide 1 (GLP-1). Molecular Metabolism 30:72–130.

[13] Taneera, J., Dhaiban, S., Mohammed, A.K., Mukhopadhyay, D., Aljaibeji, H., Sulaiman, N., et al., 2019. GNAS gene is an important regulator of insulin secretory capacity in pancreatic β-cells. Gene 715:144028.

[14] Li, Y., Cao, X., Li, L.X., Brubaker, P.L., Edlund, H., Drucker, D.J., 2005. beta-Cell Pdx1 expression is essential for the glucoregulatory, proliferative, and cytoprotective actions of glucagon-like peptide-1. Diabetes 54(2):482–491.

[15] Blanchet, E., Van de Velde, S., Matsumura, S., Hao, E., LeLay, J., Kaestner, K., et al., 2015. Feedback inhibition of CREB signaling promotes beta cell dysfunction in insulin resistance. Cell Reports 10(7):1149–1157.

[16] Wei, J., Hanna, T., Suda, N., Karsenty, G., Ducy, P., 2014. Osteocalcin promotes beta-cell proliferation during development and adulthood through Gprc6a. Diabetes 63(3):1021–1031.

[17] Andersson, O., Adams, B.A., Yoo, D., Ellis, G.C., Gut, P., Anderson, R.M., et al., 2012. Adenosine signaling promotes regeneration of pancreatic beta cells in vivo. Cell Metabolism 15(6):885–894.

[18] Ackermann, A.M., Gannon, M., 2007. Molecular regulation of pancreatic beta-cell mass development, maintenance, and expansion. Journal of Molecular Endocrinology 38(1–2):193–206.

[19] Perfetti, R., Zhou, J., Doyle, M.E., Egan, J.M., 2000. Glucagon-like peptide-1 induces cell proliferation and pancreatic-duodenum homeobox-1 expression and increases endocrine cell mass in the pancreas of old, glucose-intolerant rats. Endocrinology 141(12):4600–4605.

[20] Cornu, M., Yang, J.Y., Jaccard, E., Poussin, C., Widmann, C., Thorens, B., 2009. Glucagon-like peptide-1 protects beta-cells against apoptosis by increasing the activity of an IGF-2/IGF-1 receptor autocrine loop. Diabetes 58(8):1816–1825.

[21] Xie, T., Chen, M., Zhang, Q.H., Ma, Z., Weinstein, L.S., 2007. Beta cell-specific deficiency of the stimulatory G protein alpha-subunit Gsalpha leads to reduced beta cell mass and insulin-deficient diabetes. Proceedings of the National Academy of Sciences of the United States of America 104(49):19601–19606.

[22] Berger, M., Scheel, D.W., Macias, H., Miyatsuka, T., Kim, H., Hoang, P., et al., 2015. Galphai/o-coupled receptor signaling restricts pancreatic beta-cell expansion. Proceedings of the National Academy of Sciences of the United States of America 112(9):2888–2893.

[23] Thorens, B., Tarussio, D., Maestro, M.A., Rovira, M., Heikkila, E., Ferrer, J., 2015. Ins1(Cre) knock-in mice for beta cell-specific gene recombination. Diabetologia 58(3):558–565.

[24] Song, J., Xu, Y., Hu, X., Choi, B., Tong, Q., 2010. Brain expression of Cre recombinase driven by pancreas-specific promoters. Genesis 48(11):628–634.

[25] Brouwers, B., de Faudeur, G., Osipovich, A.B., Goyvaerts, L., Lemaire, K., Boesmans, L., et al., 2014. Impaired islet function in commonly used transgenic mouse lines due to human growth hormone minigene expression. Cell Metabolism 20(6):979–990.

[26] Chen, M., Gavrilova, O., Liu, J., Xie, T., Deng, C., Nguyen, A.T., et al., 2005. Alternative Gnas gene products have opposite effects on glucose and lipid metabolism. Proceedings of the National Academy of Sciences of the United States of America 102(20):7386–7391.

[27] Srinivas, S., Watanabe, T., Lin, C.S., William, C.M., Tanabe, Y., Jessell, T.M., et al., 2001. Cre reporter strains produced by targeted insertion of EYFP and ECFP into the ROSA26 locus. BMC Developmental Biology 1:4.

[28] Pardo, F.N., Altirriba, J., Pradas-Juni, M., Garcia, A., Ahlgren, U., Barbera, A., et al., 2012. The role of Raf-1 kinase inhibitor protein in the regulation of pancreatic beta cell proliferation in mice. Diabetologia 55(12):3331–3340.

[29] Cervantes, S., Fontcuberta-PiSunyer, M., Servitja, J.M., Fernandez-Ruiz, R., Garcia, A., Sanchez, L., et al., 2017. Late-stage differentiation of embryonic pancreatic beta-cells requires Jarid2. Scientific Reports 7(1):11643.

[30] Eriksson, A.U., Svensson, C., Hornblad, A., Cheddad, A., Kostromina, E., Eriksson, M., et al., 2013. Near infrared optical projection tomography for assessments of beta-cell mass distribution in diabetes research. Journal of Visualized Experiments 71:e50238.

[31] Alanentalo, T., Asayesh, A., Morrison, H., Loren, C.E., Holmberg, D., Sharpe, J., et al., 2007. Tomographic molecular imaging and 3D quantification within adult mouse organs. Nature Methods 4(1):31–33.

[32] Sharpe, J., Ahlgren, U., Perry, P., Hill, B., Ross, A., Hecksher-Sorensen, J., et al., 2002. Optical projection tomography as a tool for 3D microscopy and gene expression studies. Science 296(5567):541–545.

[33] Liu, J.S., Hebrok, M., 2017. All mixed up: defining roles for beta-cell subtypes in mature islets. Genes & Development 31(3):228–240.

[34] Huang, C., Walker, E.M., Dadi, P.K., Hu, R., Xu, Y., Zhang, W., et al., 2018. Synaptotagmin 4 regulates pancreatic beta cell maturation by modulating the Ca(2+) sensitivity of insulin secretion vesicles. Developmental Cell 45(3): 347–361 e345.

[35] Shin, S., Le Lay, J., Everett, L.J., Gupta, R., Rafiq, K., Kaestner, K.H., 2014. CREB mediates the insulinotropic and anti-apoptotic effects of GLP-1 signaling in adult mouse beta-cells. Molecular Metabolism 3(8):803–812.

[36] Song, W.J., Schreiber, W.E., Zhong, E., Liu, F.F., Kornfeld, B.D., Wondisford, F.E., et al., 2008. Exendin-4 stimulation of cyclin A2 in beta-cell proliferation. Diabetes 57(9):2371–2381.

[37] Greenwood, M.P., Rahman, P.A., Gillard, B.T., Langley, S., Iwasaki, Y., et al., 2020. Transcription factor Creb3l1 regulates the synthesis of prohormone convertase enzyme PC1/3 in endocrine cells. Journal of Neuroendocrinology 32:e12851.

[38] Cheng, X., Ji, Z., Tsalkova, T., Mei, F., 2008. Epac and PKA: a tale of two intracellular cAMP receptors. Acta Biochimica et Biophysica Sinica (Shanghai) 40(7):651–662.

[39] Borland, G., Smith, B.O., Yarwood, S.J., 2009. EPAC proteins transduce diverse cellular actions of cAMP. British Journal of Pharmacology 158(1):70–86.

[40] Goodyer, W.R., Gu, X., Liu, Y., Bottino, R., Crabtree, G.R., Kim, S.K., 2012. Neonatal beta cell development in mice and humans is regulated by calcineurin/NFAT. Developmental Cell 23(1):21–34.

[41] Trumper, J., Ross, D., Jahr, H., Brendel, M.D., Goke, R., Horsch, D., 2005. The Rap-B-Raf signalling pathway is activated by glucose and glucagon-like peptide-1 in human islet cells. Diabetologia 48(8):1534–1540.

[42] Dalle, S., Quoyer, J., Varin, E., Costes, S., 2011. Roles and regulation of the transcription factor CREB in pancreatic beta -cells. Current Molecular Pharmacology 4(3):187–195.

[43] Stewart, A.F., Hussain, M.A., Garcia-Ocana, A., Vasavada, R.C., Bhushan, A., Bernal-Mizrachi, E., et al., 2015. Human b-cell proliferation and intracellular signaling. Diabetes 64(6):14.

[44] Ueki, K., Okada, T., Hu, J., Liew, C.W., Assmann, A., Dahlgren, G.M., et al., 2006. Total insulin and IGF-I resistance in pancreatic beta cells causes overt diabetes. Nature Genetics 38(5):583–588.

[45] Kulkarni, R.N., Bruning, J.C., Winnay, J.N., Postic, C., Magnuson, M.A., Kahn, C.R., 1999. Tissue-specific knockout of the insulin receptor in pancreatic beta cells creates an insulin secretory defect similar to that in type 2 diabetes. Cell 96(3):329–339.

[46] Kubota, N., Terauchi, Y., Tobe, K., Yano, W., Suzuki, R., Ueki, K., et al., 2004. Insulin receptor substrate 2 plays a crucial role in beta cells and the hypothalamus. Journal of Clinical Investigation 114(7):917–927.

[47] Cantley, J., Choudhury, A.I., Asare-Anane, H., Selman, C., Lingard, S., Heffron, H., et al., 2007. Pancreatic deletion of insulin receptor substrate 2 reduces beta and alpha cell mass and impairs glucose homeostasis in mice. Diabetologia 50(6):1248–1256.

[48] Cornu, M., Modi, H., Kawamori, D., Kulkarni, R.N., Joffraud, M., Thorens, B., 2010. Glucagon-like peptide-1 increases beta-cell glucose competence and proliferation by translational induction of insulin-like growth factor-1 receptor expression. Journal of Biological Chemistry 285(14):10538–10545.

[49] Jhala, U.S., Canettieri, G., Screaton, R.A., Kulkarni, R.N., Krajewski, S., Reed, J., et al., 2003. cAMP promotes pancreatic beta-cell survival via CREB-mediated induction of IRS2. Genes & Development 17(13):1575–1580.

[50] Wittenberg, A.D., Azar, S., Klochendler, A., Stolovich-Rain, M., Avraham, S., Birnbaum, L., et al., 2016. Phosphorylated ribosomal protein S6 is required for Akt-driven hyperplasia and malignant transformation, but not for hypertrophy, Aneuploidy and hyperfunction of pancreatic beta-cells. PloS One 11(2):e0149995.

[51] Araujo, E.P., Amaral, M.E., Souza, C.T., Bordin, S., Ferreira, F., Saad, M.J., et al., 2002. Blockade of IRS1 in isolated rat pancreatic islets improves glucose-induced insulin secretion. FEBS Letters 531(3): 437–442.

[52] Otani, K., Kulkarni, R.N., Baldwin, A.C., Krutzfeldt, J., Ueki, K., Stoffel, M., et al., 2004. Reduced beta-cell mass and altered glucose sensing impair insulin-secretory function in betaIRKO mice. American Journal of Physiology. Endocrinology and Metabolism 286(1):E41–E49.

[53] Belfiore, A., Malaguarnera, R., Vella, V., Lawrence, M.C., Sciacca, L., Frasca, F., et al., 2017. Insulin receptor isoforms in physiology and disease: an updated view. Endocrine Reviews 38(5):53.

[54] Pamir, N., Lynn, F.C., Buchan, A.M., Ehses, J., Hinke, S.A., Pospisilik, J.A., et al., 2003. Glucose-dependent insulinotropic polypeptide receptor null mice exhibit compensatory changes in the enteroinsular axis. American Journal of Physiology. Endocrinology and Metabolism 284(5):E931–E939.

[55] Hansotia, T., Baggio, L.L., Delmeire, D., Hinke, S.A., Yamada, Y., Tsukiyama, K., et al., 2004. Double incretin receptor knockout (DIRKO) mice reveal an essential role for the enteroinsular axis in transducing the glucoregulatory actions of DPP-IV inhibitors. Diabetes 53(5):1326–1335.

[56] Flamez, D., Van Breusegem, A., Scrocchi, L.A., Quartier, E., Pipeleers, D., Drucker, D.J., et al., 1998. Mouse pancreatic beta-cells exhibit preserved glucose competence after disruption of the glucagon-like peptide-1 receptor gene. Diabetes 47(4):646–652.

[57] Campbell, J.E., Ussher, J.R., Mulvihill, E.E., Kolic, J., Baggio, L.L., Cao, X., et al., 2016. TCF1 links GIPR signaling to the control of beta cell function and survival. Nature Medicine 22(1):84–90.

[58] Panaro, B.L., Flock, G.B., Campbell, J.E., Beaudry, J.L., Cao, X., Drucker, D.J., 2017. Beta-cell inactivation of Gpr119 unmasks incretin dependence of GPR119-mediated glucoregulation. Diabetes 66(6):1626–1635.

[59] Martin, B., Shin, Y.K., White, C.M., Ji, S., Kim, W., Carlson, O.D., et al., 2010. Vasoactive intestinal peptide-null mice demonstrate enhanced sweet taste preference, dysglycemia, and reduced taste bud leptin receptor expression. Diabetes 59(5):1143–1152.

[60] Hang, Y., Yamamoto, T., Benninger, R.K.P., Brissova, M., Guo, M., Bush, W., et al., 2014. The MafA transcription factor becomes essential to islet β-cells soon after birth. Diabetes 63(6):1994–2005.

[61] Nishimura, W., Takahashi, S., Yasuda, K., 2015. MafA is critical for maintenance of the mature beta cell phenotype in mice. Diabetologia 58(3): 566–574.

[62] Aramata, S., Han, S.-L., Kataoka, K., 2007. Roles and regulation of transcription factor MafA in islet beta-cells. Endocrine Journal 54(5):659–666.

[63] Dai, C., Hang, Y., Shostak, A., Poffenberger, G., Hart, N., Prasad, N., et al., 2017. Age-dependent human beta cell proliferation induced by glucagon-like peptide 1 and calcineurin signaling. Journal of Clinical Investigation 127(10): 3835–3844.

[64] Rhodes, C.J., White, M.F., Leahy, J.L., Kahn, S.E., 2013. Direct autocrine action of insulin on beta-cells: does it make physiological sense? Diabetes 62(7):2157–2163.

[65] Rachdaoui, N., 2020. Insulin: the friend and the foe in the development of type 2 diabetes mellitus. International Journal of Molecular Sciences 21(5).

[66] Belfiore, A., Frasca, F., Pandini, G., Sciacca, L., Vigneri, R., 2009. Insulin receptor isoforms and insulin receptor/insulin-like growth factor receptor hybrids in physiology and disease. Endocrine Reviews 30(6):586–623.

[67] Malakar, P., Chartarifsky, L., Hija, A., Leibowitz, G., Glaser, B., Dor, Y., et al., 2016. Insulin receptor alternative splicing is regulated by insulin signaling and modulates beta cell survival. Scientific Reports 6:31222.

